THE JOURNAL OF PHYSICAL CHEMISTRY Letters

Letter

pubs.acs.org/JPCL

Preparation of Single-Phase Films of $CH_3NH_3Pb(I_{1-x}Br_x)_3$ with Sharp Optical Band Edges

Aditya Sadhanala,[†] Felix Deschler,[†] Tudor H. Thomas,[†] Siân E. Dutton,[†] Karl C. Goedel,[†] Fabian C. Hanusch,[‡] May L. Lai,[†] Ullrich Steiner,[†] Thomas Bein,[‡] Pablo Docampo,[‡] David Cahen,[§] and Richard H. Friend*,[†]

[†]Cavendish Laboratory, JJ Thomson Avenue, Cambridge CB3 0HE, United Kingdom

[‡]Ludwig-Maximilians-Universität München, Butenandtstraße 11, 81377 München, Germany

[§]Department of Materials and Interfaces, Weizmann Institute of Science, Rehovot 76100, Israel

Supporting Information

ABSTRACT: Organometallic lead-halide perovskite-based solar cells now approach 18% efficiency. Introducing a mixture of bromide and iodide in the halide composition allows tuning of the optical bandgap. We prepare mixed bromide−iodide lead perovskite films $CH_3NH_3Pb(I_{1-x}Br_x)_3$ ($0 \le x \le 1$) by spin-coating from solution and obtain films with monotonically varying bandgaps across the full composition range. Photothermal deflection spectroscopy, photoluminescence, and X-ray diffraction show that following suitable fabrication protocols these mixed lead-halide perovskite films form a single phase. The optical absorption edge of the pure triiodide and tribromide perovskites is sharp with Urbach energies of 15 and 23 meV, respectively, and reaches a maximum of 90 meV for $CH_3NH_3PbI_{1.2}Br_{1.8}$. We demonstrate a bromide−iodide lead perovskite film ($CH_3NH_3PbI_{1.2}Br_{1.8}$) with an optical bandgap of 1.94 eV, which is optimal for tandem cells of these materials with crystalline silicon devices.

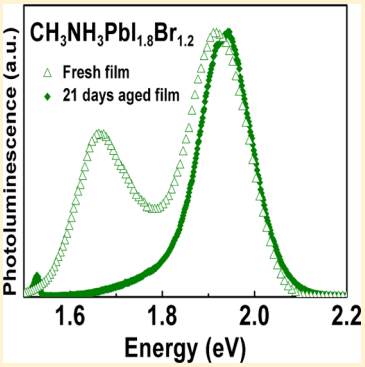

SECTION: Energy Conversion and Storage; Energy and Charge Transport

Solution processable optoelectronic devices offer cost-effective, large-scale manufacturing capability. Hybrid organic−inorganic perovskite ($CH_3NH_3PbI_{3-x}Cl_x$) solar cells now show photovoltaic (PV) performance[1−4] approaching 18%,[5,6] and high charge-carrier mobilities.[7] Perovskite films have also shown promising photoluminescence quantum efficiencies (PLQEs) of more than 70% and lasing, making them a promising candidate for cost-effective and efficient LEDs and lasing applications.[8,9] Despite the rapid progress in the past few years, relatively little is known about the properties required for efficient perovskite PV systems or why perovskite works so well in PVs while simultaneously demonstrating high PLQE. It has recently been demonstrated by Noh et al. that the bandgap of the perovskite can be tuned by varying the halide (i.e., bromide, iodide) composition of the perovskite precursor solution.[10,11] High open-circuit voltages have been demonstrated by using the higher bandgap tribromide-based perovskite.[12−14]

The control of bandgap with mixed halide systems is attractive, but it is important to establish whether these form solid solutions, with monotonic variation of lattice constants and bandgap, or if there is compositional inhomogeneity, which may introduce a range of local bandgaps and reduce PV performance. To address this question, we use photothermal deflection spectroscopy (PDS) and photoluminescence measurements that are able to detect low levels of subgap states in the system $CH_3NH_3Pb(I_{1-x}Br_x)_3$ ($0 \le x \le 1$). We correlate our findings with the structural information obtained by X-ray diffraction (XRD) measurements. We find that films of mixed trihalide perovskites initially form a system with two absorption and luminescence features. Following our fabrication protocol, these convert to a homogeneous intermixed system with only one species within the detection limits of the techniques used in this work. The ability to engineer a single bandgap in these mixed compositions is important for the development of solar cells. We demonstrate a bromide−iodide lead perovskite film ($CH_3NH_3PbI_{1.2}Br_{1.8}$) with an optical bandgap of 1.94 eV, which is optimal for tandem cell applications with c-Si cells. Our findings also show that pure trihalide perovskites have a remarkably low energetic disorder, which is, to our knowledge, by far the lowest reported for any low temperature solution-processable material.[15,16]

PDS is an ultrasensitive absorption measurement technique that detects heating of the sample due to the nonradiative relaxation of absorbed light and is insensitive to reflection and scattering. PDS can be used to characterize energetic disorder as the exponential decay of the absorption below the bandgap with a characteristic energy, the Urbach energy (E_u), and has been used to study the perovskite materials system.[16] The

Received: June 27, 2014
Accepted: July 9, 2014
Published: July 9, 2014

   dx.doi.org/10.1021/jz501332v | J. Phys. Chem. Lett. 2014, 5, 2501−2505

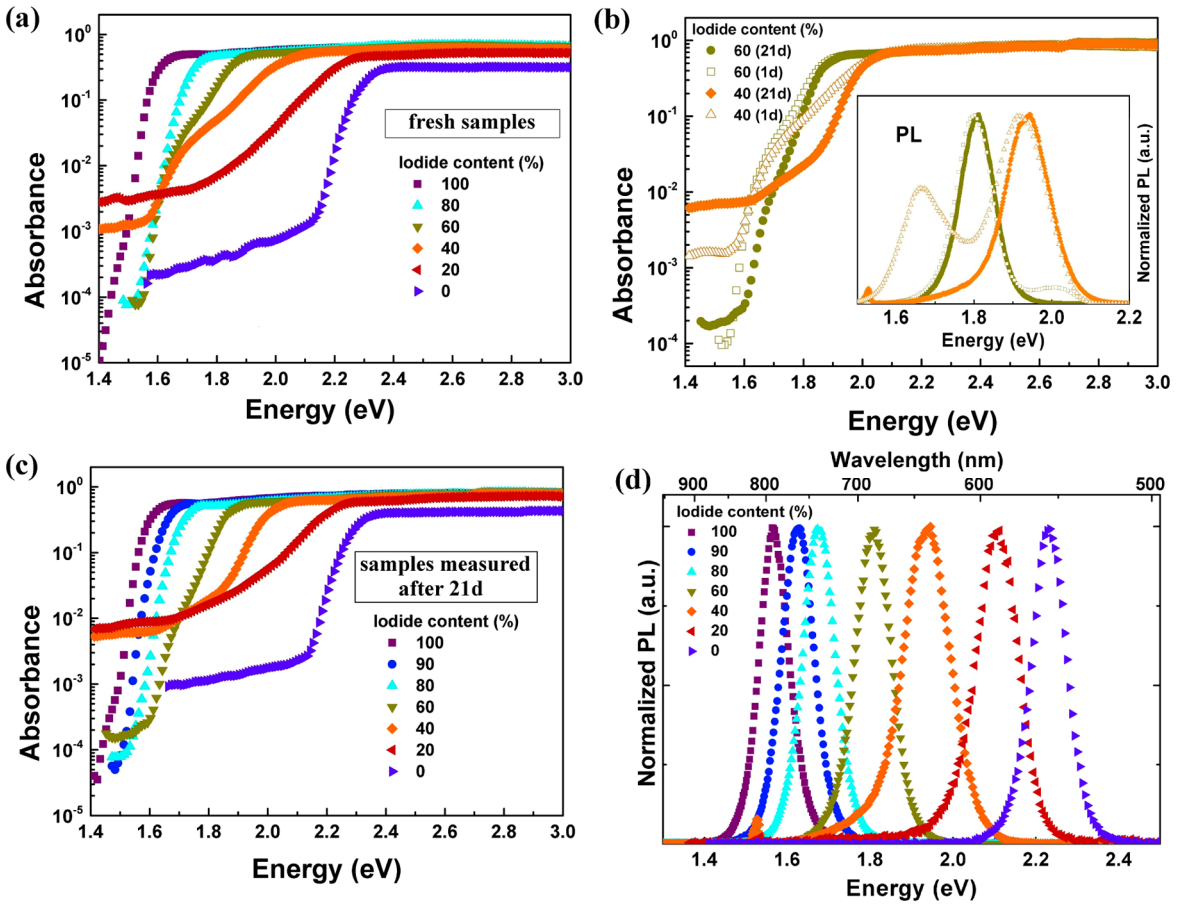

Figure 1. (a,c) PDS measurements for 1:1 molar methylammonium lead-halide thin films with different iodide–bromide ratios, as indicated, measured directly after fabrication (a) and 21 days later (c). (b) Change in PDS spectrum for films measured on the same day after annealing and after 21 days. Inset shows the corresponding change in the PL spectra. (d) PL spectra of 1:1 molar methylammonium lead-halide thin films with different iodide–bromide ratios, as indicated, measured after 21 days. Excitation for PL was performed with a pulsed laser system at 3.1 eV photon energy with fluence ~1 $\mu J/cm^2$ and 100 fs pulse length. PL spectra have been normalized to the peak emission.

Urbach energy is given by $A(E) \propto e^{E/(E_u)}$, where A is the absorbance and E is the excitation energy in electronvolts. In Figure S1 (SI), the linear fit to the Urbach tail in the PDS data for the pure triiodide perovskite is shown, which yields an Urbach energy of ~15 meV that is similar to that obtained by De Wolf et al.[16] This value is about twice the typical value for single-crystal GaAs and half that of polycrystalline CIGS.[15,17]

We prepared perovskite thin films by spin-coating from a precursor solution composed of 1:1 organic to inorganic ratios (CH_3NH_3I to PbI_2 and CH_3NH_3Br to $PbBr_2$) under a N_2 atmosphere in a glovebox (details in the SI). Solutions with varying iodide to bromide concentration were prepared by mixing the respective pure triiodide ($CH_3NH_3PbI_3$) and tribromide ($CH_3NH_3PbBr_3$) precursor solution in the respective ratios. Energy-dispersive X-ray spectroscopy (EDX) measurements show that the ratios of bromide to iodide in the film are the same as those in the solution (see Figure S4 and Table 1, SI). By increasing the concentration of the pure triiodide perovskite in the tribromide perovskite in solution from 0 to 100%, we tune the bandgap of the resulting perovskite between the extremes of pure triiodide and tribromide perovskites from 2.23 to 1.57 eV (Figure 1a,c). We detect the absorption edge of the pure triiodide lead perovskite $CH_3NH_3PbI_3$ down to the detection limit of the PDS setup without observing a leveling off, which indicates a very clean bandgap and sharp band edge. This very clean gap is preserved as bromide is added up to 20% bromide (80% iodide) content. For the pure tribromide perovskite, $CH_3NH_3PbBr_3$, a sharp band edge with additional levels of sub-bandgap absorption is found, which indicates a population of sub-bandgap states. The absorption edge for films with 20% iodide shows a broad absorption tail below the band edge and significant sub-bandgap absorption below ~1.8 eV. We interpret this as increased disorder in these films and a significant population of sub-bandgap states. Notably, for iodide–bromide mixtures with 40 and 60% iodide content, the films show a clear shoulder in the subgap absorption (Figure 1b). We interpret this as the initial formation of two species in these films. Photoluminescence (PL) measurements of the bromide–iodide lead perovskite films with 40 and 60% iodide content show two emission peaks (Figure 1b inset). Time-resolved PL measurements (Figure 2a,b) show that the higher energy emission band decays more rapidly than the lower energy band. These findings suggest that the initially formed mixed-halide perovskite films, having 40 and 60% iodide content, comprise two species. We note, in particular, that for the 40% iodide films the second phase emits around 1.68 eV from a significantly lower energy than the 1.94 eV emissive feature, and this represents a potential loss mechanism for PV devices.

Surprisingly, we found that the PDS absorption and PL spectra changed after the films were stored under an inert

dx.doi.org/10.1021/jz501332v | J. Phys. Chem. Lett. 2014, 5, 2501–2505

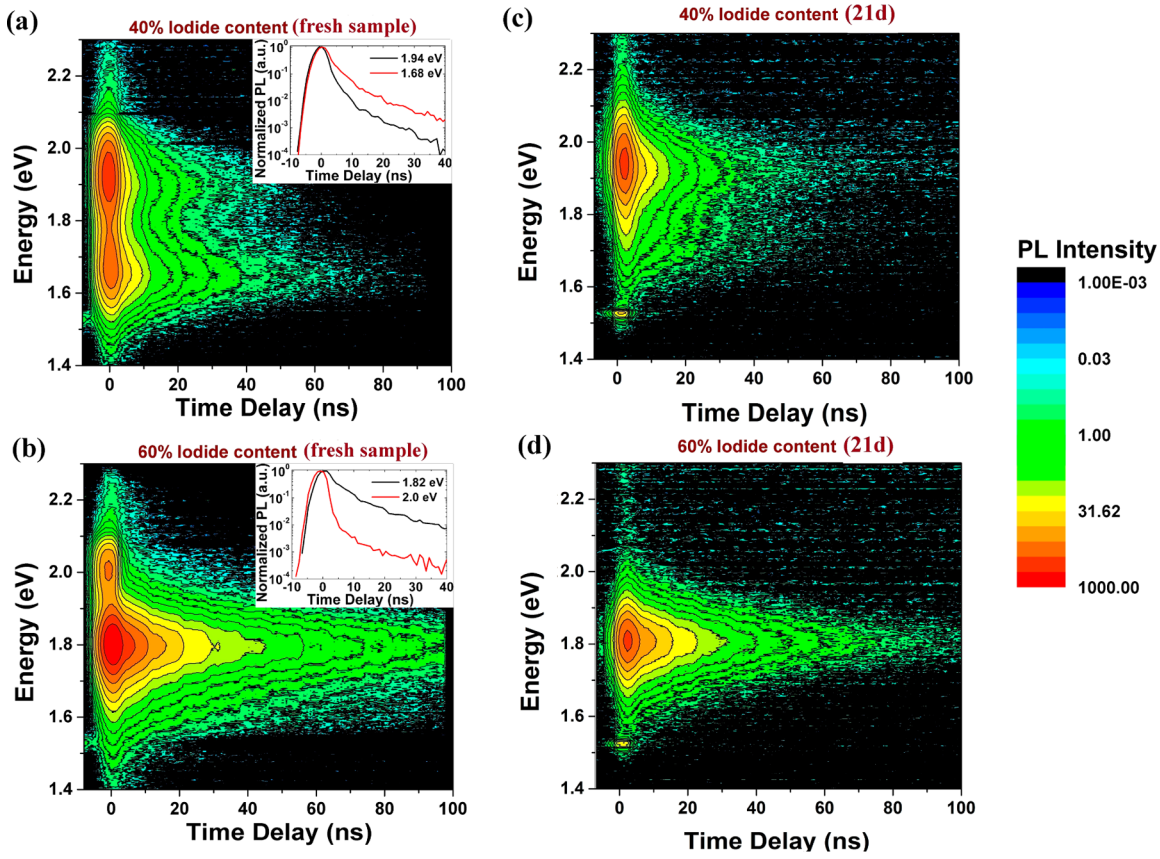

Figure 2. Plot of PL intensity versus time and emission wavelength for 1:1 molar methylammonium halide–lead-halide films with an iodide content of 40 (a,c) and 60% (b,d) fresh samples and remeasured after 21 days. Inset in panels a and b shows the kinetics of the respective PL peaks at the stated energies. Excitation for PL was performed with a pulsed laser system at 3.1 eV photon energy with fluence ~1 μJ/cm^2 and 100 fs pulse length.

nitrogen atmosphere at room temperature (these changes were complete within 3 weeks and showed no significant further evolution at 13 weeks) (Figure 1b). A similar effect was observed in fresh films prepared from solutions that had been kept at room temperature for several days (see Figure S2, SI). The most striking changes in the PDS spectra in these aged films, which we term here "single-phase" films, is the sharpening of the band edges and the loss of the extra absorption shoulder in the subgap.

In detail, in the as-formed films with low iodide contents (20 and 40%), made from fresh solutions, we find additional sub-bandgap absorption and broadened band edges. However, there is no longer a second phase detectable within the resolution of the PDS setup if the films are allowed to age or are made from aged solutions. For all other iodide contents (0, 80, 90, and 100%), the PDS absorption spectra show sharp band edges and little differences compared with the films measured directly after preparation. The steady-state PL spectra of the "single phase" films (Figure 1d) show single transitions with a monotonic shift in peak position with increasing iodide content from pure tribromide perovskite (2.23 eV) to pure triiodide perovskite (1.57 eV). This finding supports our observation of a clean bandgap in these films. The photoluminescence kinetics (Figure 3d) show single bimolecular decays for the pure iodide and bromide films and also for iodide-rich films down to 60% iodide, as reported previously for the iodide material.[9] Films with 20 and 40% iodide content both show fast kinetics. These findings also point toward one photoactive species from which emission arises in the bromide–iodide lead perovskite films. Time-resolved PL spectra of "single-phase" films also show one emissive species (Figure 2c,d).

Figure 3c shows the full width at half-maximum (fwhm) of the PL peaks together with the Urbach energy calculated from PDS measurements. (For details about the fits used for calculating the Urbach energies, see Figure S7 in the SI.) Both parameters follow similar trends, peaking below 50% iodide content. We take this observation as an indication that absorption and emission arise from similar states. We find that the pure tribromide perovskite films and films with 100 to 80% of iodide content show the lowest fwhm and the lowest Urbach energies. This indicates very low disorder and sharp band edges in the films with higher iodide content compared with the ones with lower iodide content. Also, the larger fwhm and Urbach energies for films with 20 and 40% than for those with higher iodide content correlate with shorter lifetimes observed in transient PL (Figure 3d). However, when we compare the PL peak positions with the PDS absorption data, we find that the emission peaks for all films lie at the energy where the absorption has dropped to ~15% of its maximum band edge value. (See Figure S5 in the SI.) First, this indicates that impurity levels at lower energy do not play a significant role in the radiative recombination of excited states. Therefore, they do not represent a major radiative form of energetic loss channel due to energy relaxation down to the lower lying states within the subgap. Moreover, the lower subgap absorption detected for "single-phase" films suggests a lower density of states that recombine through nonradiative relaxation, which again indicates a cleaner material system.

dx.doi.org/10.1021/jz501332v | J. Phys. Chem. Lett. 2014, 5, 2501–2505

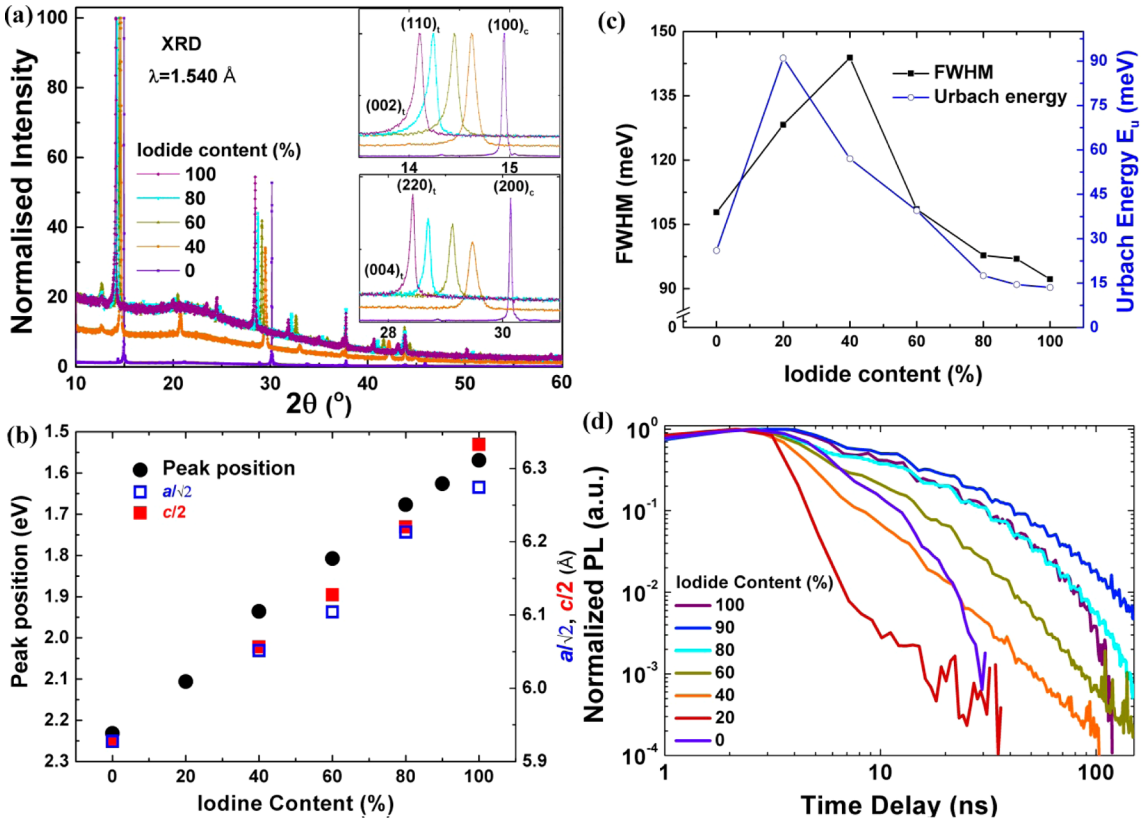

Figure 3. (a) Intensity-normalized X-ray diffraction patterns of 1:1 molar methylammonium lead-halide thin films with different iodide-bromide ratios, as indicated. The evolution of the position of the $(002)_t$ and $(110)_t$ [$(100)_c$] and the $(004)_t$ and $(220)_t$ [$(200)_c$] peaks as a function of composition are shown in the upper and lower insets, respectively. (b) Variation of PL peak positions (closed circles) and normalized lattice parameters $a/\sqrt{2}$ (open squares) and $c/2$ (closed squares) determined from XRD measurements for films with different iodide content. (c) Comparison of the change in fwhm of the PL emission peak and the Urbach energy calculated from PDS measurements for the same films measured after 21 days. (d) Plot of normalized PL intensity versus time for same films. Excitation for PL was performed with a pulsed laser system at 3.1 eV photon energy with fluence ~1 μJ/cm^2 and 100 fs pulse length.

Powder X-ray diffraction measurements were carried out on "single phase" films over the entire composition range (Figure 3a). A systematic shift in the patterns to lower scattering angles is observed as the concentration of iodide increases, indicating an expansion of the unit cell with increasing iodide fraction. Because of preferential alignment in the films, a complete structural analysis was not possible. The symmetry and lattice parameters were modeled using a Le Bail analysis[18] in the Fullprof suite of programmes (see Figure S6, SI).[19] The characteristic perovskite peak at $2\theta = 30°$ (Figure 3a, inset) shows a significant broadening of the $(200)_c$ reflection in all films containing iodide. We ascribe this to a tetragonal distortion and the emergence of two unique reflections, $(002)_t$ and $(110)_t$; a similar although less pronounced splitting is also observed in the $(100)_c$ reflection with iodide present (Figure 3a, inset). Therefore, with the exception of the pure bromide film, all films were modeled using a tetragonal unit cell with *I4cm* symmetry, as has previously been reported for $CH_3NH_3PbI_3$.[20] The pure bromide film was modeled using a higher symmetry $Pm\bar{3}m$ cubic structure.[20] In all films, unreacted starting materials of CH_3NH_3X and PbX_2 were detected in addition to the main perovskite phase. The unit cell of the tetragonal phase, a_t and c_t, can be related to that of the cubic cell, a_c, by $a_t = \sqrt{2}a_c$ and $c_t = 2a_c$. When the cell parameters of the tetragonal cell are normalized, $a_t/\sqrt{2}$, $c_t/2$, to allow for direct comparison to the cubic perovskite structure, a linear increase in the size of the normalized unit cell with increasing iodide fraction is observed (Figure 3b). This is consistent with both the larger ionic radii of iodide (r = 2.2 Å) with respect to bromide (r = 1.96 Å) and Vegard's law for a continuous solid solution. The degree of tetragonal distortion, $((c_t - \sqrt{2}a_t)/((a_t/\sqrt{2}) + (c_t/2)))$, also increases with iodide concentration reaching a maximum value of 0.9% in $CH_3NH_3PbI_3$. An additional broadening of reflections in the mixed halide films is observed (Figure 3a, inset), which cannot be described as resulting only from changes in the symmetry. We attribute this to strain broadening. Strain of this type could be due to quenching of a higher temperature (cubic) symmetry phase or could arise from an inhomogeneous halide distribution beyond random site occupancy. Since submission, we became aware of a report by Park et al.,[21] where changes in the crystallinity, microstructure and preferential alignment are observed in films of $CH_3NH_3PbI_{3-x}Cl_x$ and $CH_3NH_3PbI_3$ aged over five weeks.

In Figure 3b, we compare the extracted normalized lattice parameters with the optically determined PL peak positions. Both lattice parameters and PL peak energies follow a linear trend with iodide fraction. These observations support our finding that there is a single solid solution across the full composition range that can be obtained using a straightforward fabrication protocol. This protocol requires "aging" of either the starting solution or the as-prepared films. The underlying reason for the observed effect is currently under investigation.

Our demonstration of remarkably clean bromide/iodide solid solutions in this organometallic halide PV system brings this

dx.doi.org/10.1021/jz501332v | J. Phys. Chem. Lett. 2014, 5, 2501−2505

remarkable family of materials in line with classic semiconductor systems such as MBE-grown III-Vs including AlGaAs.

■ ASSOCIATED CONTENT

Supporting Information

Additional figures, including EDX, PDS absorption spectra, Le Bail fits, Urbach tail fits for calculation of Urbach energies, and details about sample fabrication and experimental techniques used. This material is available free of charge via the Internet at http://pubs.acs.org

■ AUTHOR INFORMATION

Corresponding Author

*E-mail: rhf10@cam.ac.uk.

Notes

The authors declare no competing financial interests.

■ ACKNOWLEDGMENTS

We thank Prof. Henry Snaith, Dr. Antonio Abate, Dr. Sandeep Pathak, and Mr. Giles Eperon for insightful discussions on the results and sample fabrication. We acknowledge funding from the Engineering and Physical Sciences Research Council (EPSRC) and the Winton Programme (Cambridge) for the Physics of Sustainability. T.H.T. acknowledges funding from Cambridge Australia Scholarships and the Cambridge Commonwealth Trust. D.C. acknowledges support from St. John's College Cambridge and the Winton Programme (Cambridge) for the Physics of Sustainability.

■ REFERENCES

(1) Ball, J. M.; Lee, M. M.; Hey, A.; Snaith, H. J. Low-Temperature Processed Meso-Superstructured to Thin-Film Perovskite Solar Cells. *Energy Environ. Sci.* **2013**, *6*, 1739−1743.

(2) Kim, H.-S.; Lee, C.-R.; Im, J.-H.; Lee, K.-B.; Moehl, T.; Marchioro, A.; Moon, S.-J.; Humphry-Baker, R.; Yum, J.-H.; Moser, J. E.; et al. Lead Iodide Perovskite Sensitized All-Solid-State Submicron Thin Film Mesoscopic Solar Cell with Efficiency Exceeding 9%. *Sci. Rep.* **2012**, *2*, 591−598.

(3) Liu, M.; Johnston, M. B.; Snaith, H. J. Efficient Planar Heterojunction Perovskite Solar Cells by Vapour Deposition. *Nature* **2013**, *501*, 395−398.

(4) Snaith, H. J. Perovskites: The Emergence of a New Era for Low-Cost, High-Efficiency Solar Cells. *J. Phys. Chem. Lett.* **2013**, *4*, 3623−3630.

(5) National Renewable Energy Laboratory. Efficiency chart http://www.nrel.gov/ncpv/images/efficiency_chart.jpg.

(6) Green, M. A.; Ho-Baillie, A.; Snaith, H. J. The Emergence of Perovskite Solar Cells. *Nat. Photonics* **2014**, *8*, 506−514.

(7) Wehrenfennig, C.; Eperon, G. E.; Johnston, M. B.; Snaith, H. J.; Herz, L. M. High Charge Carrier Mobilities and Lifetimes in Organolead Trihalide Perovskites. *Adv. Mater.* **2014**, *26*, 1584−1589.

(8) Xing, G.; Mathews, N.; Lim, S. S.; Yantara, N.; Liu, X.; Sabba, D.; Grätzel, M.; Mhaisalkar, S.; Sum, T. C. Low-Temperature Solution-Processed Wavelength-Tunable Perovskites for Lasing. *Nat. Mater.* **2014**, *13*, 476−480.

(9) Deschler, F.; Price, M.; Pathak, S.; Klintberg, L. E.; Jarausch, D.-D.; Higler, R.; Hüttner, S.; Leijtens, T.; Stranks, S. D.; Snaith, H. J.; et al. High Photoluminescence Efficiency and Optically Pumped Lasing in Solution-Processed Mixed Halide Perovskite Semiconductors. *J. Phys. Chem. Lett.* **2014**, *5*, 1421−1426.

(10) Noh, J. H.; Im, S. H.; Heo, J. H.; Mandal, T. N.; Seok, S. Il. Chemical Management for Colorful, Efficient, and Stable Inorganic-Organic Hybrid Nanostructured Solar Cells. *Nano Lett.* **2013**, *13*, 1764−1769.

(11) Eperon, G. E.; Stranks, S. D.; Menelaou, C.; Johnston, M. B.; Herz, L. M.; Snaith, H. J. Formamidinium Lead Trihalide: A Broadly Tunable Perovskite for Efficient Planar Heterojunction Solar Cells. *Energy Environ. Sci.* **2014**, *7*, 982−988.

(12) Edri, E.; Kirmayer, S.; Cahen, D.; Hodes, G. High Open-Circuit Voltage Solar Cells Based on Organic−Inorganic Lead Bromide Perovskite. *J. Phys. Chem. Lett.* **2013**, *4*, 897−902.

(13) Edri, E.; Kirmayer, S.; Kulbak, M.; Hodes, G.; Cahen, D. Chloride Inclusion and Hole Transport Material Doping to Improve Methyl Ammonium Lead Bromide Perovskite-Based High Open-Circuit Voltage Solar Cells. *J. Phys. Chem. Lett.* **2014**, *5*, 429−433.

(14) Ryu, S.; Noh, J. H.; Jeon, N. J.; Kim, Y. C.; Yang, W. S.; Seo, J. W.; Seok, S. Il. Voltage Output of Efficient Perovskite Solar Cells with High Open-Circuit Voltage and Fill Factor. *Energy Environ. Sci.* **2014**, DOI: 10.1039/C4EE00762J.

(15) Heath, J. T.; Cohen, J. D.; Shafarman, W. N.; Liao, D. X.; Rockett, A. A. Effect of Ga Content on Defect States in $CuIn_{1-x}Ga_xSe_2$ Photovoltaic Devices. *Appl. Phys. Lett.* **2002**, *80*, 4540−4542.

(16) De Wolf, S.; Holovsky, J.; Moon, S.-J.; Löper, P.; Niesen, B.; Ledinsky, M.; Haug, F.-J.; Yum, J.-H.; Ballif, C. Organometallic Halide Perovskites: Sharp Optical Absorption Edge and Its Relation to Photovoltaic Performance. *J. Phys. Chem. Lett.* **2014**, *5*, 1035−1039.

(17) Miller, O. D.; Yablonovitch, E.; Kurtz, S. R. Strong Internal and External Luminescence as Solar Cells Approach the Shockley−Queisser Limit. *IEEE J. Photovoltaics* **2012**, *2*, 303−311.

(18) Le Bail, A.; Duroy, H.; Fourquet, J. L. Ab-Initio Structure Determination of $LiSbWO_6$ by X-Ray Powder Diffraction. *Mater. Res. Bull.* **1988**, *23*, 447−452.

(19) Rodriguez-Carvajal, J.; Fernandez-Diaz, M. T.; Martinez, J. L. Neutron Diffraction Study on Structural and Magnetic Properties of La_2NiO_4. *J. Phys.: Condens. Matter* **1991**, *3*, 3215−3234.

(20) Poglitsch, A.; Weber, D. Dynamic Disorder in Methylammoniumtrihalogenoplumbates (II) Observed by Millimeter-Wave Spectroscopy. *J. Chem. Phys.* **1987**, *87*, 6373−6378.

(21) Park, B.-W.; Johansson, E. M. J.; Philippe, B.; Gustafsson, T.; Sveinbjörnsson, K.; Hagfeldt, A.; Boschloo, G. Enhanced Crystallinity in Organic-Inorganic Lead Halide Perovskites on Mesoporous TiO_2 via Disorder-Order Phase Transition. *Chem. Mater.* **2014**, DOI: 10.1021/cm501541p.

■ NOTE ADDED AFTER ASAP PUBLICATION

This paper was published ASAP on July 10, 2014. Minor revisions were made to the main text. The revised paper was reposted on July 17, 2014.